Materials and Design 32 (2011) 2749–2755

Contents lists available at ScienceDirect

Materials and Design

journal homepage: www.elsevier.com/locate/matdes

Microstructural and mechanical properties of friction stir welded Cu–30Zn brass alloy at various feed speeds: Influence of stir bands

M. Sarvghad Moghaddam [a,*], R. Parvizi [a], M. Haddad-Sabzevar [a], A. Davoodi [b]

[a] Metallurgical and Materials Engineering Department, Ferdowsi University of Mashhad, Mashhad 91775-1111, Iran
[b] Materials Engineering Department, Sabzevar Tarbiat Moallem University, Sabzevar 391, Iran

ARTICLE INFO

Article history:
Received 6 September 2010
Accepted 5 January 2011
Available online 18 January 2011

Keywords:
D. Welding
E. Mechanical
F. Microstructure

ABSTRACT

In this study, the effect of various feed speeds on microstructure and mechanical properties of friction stir welded Cu–30Zn brass alloy is investigated. Rotation speed was fixed at 950 rpm and feed speed varied in the range of 190–375 mm/min. Examination of the microstructure showed very fine grains with some deformed grains in the stirred zone and some coarser grains in the thermo-mechanically affected zone and base metal. A unique deformation pattern, namely "stir band" in the stirred zone region was identified and its density increased by increase in feed speed. Results showed that the grain size profile was independent of feed speed and the hardness values decreased by increase in feed speed. Increase in feed speed led to a slight improvement of yield strength and ultimate tensile strength, associated to continuous spring-like morphology of stir bands acting as a strengthening structure. However, ductility reduces considerably from 57 to 27%. Moreover, it is observed that during tensile test, fracture cracks originate exactly adjacent to the stir bands.

1. Introduction

Friction stir welding (FSW) has been successfully used to weld similar and dissimilar cast and wrought aluminum alloys, steels, as well as titanium, copper and magnesium alloys, dissimilar metal group alloys and metal matrix composites. The technique can be used to produce butt, corner, lap, T, spot and fillet joints as well as to weld hollow objects, such as tanks and tube/pipe, and parts with 3-dimensional contours [1–2]. Welding of copper is usually difficult by conventional fusion welding techniques due to the deteriorative influence of oxygen, impurities and also because of its high thermal diffusivity which is about 10–100 times higher than that of steels and nickel alloys [3–6]. In other words, the greater dissipation of heat through copper work-piece requires higher heat input for welding in comparison with other materials, resulting in quite low welding speeds [7]. Few researches have been already conducted on the FSW of copper and copper alloys [8–10]. Recently, several attempts have been made to join successfully pure copper and Cu–Zn alloys by FSW process [6–13]. Similar to other materials, four microstructural regions could be identified in FSW of copper alloys: nugget or stirred zone (SZ), thermo-mechanically affected zone (TMAZ), heat affected zone (HAZ) and base metal [6–12]. The SZ microstructure contains equiaxed and small recrystallized grains. Depending on the grain size of the base metal, its hardness may be higher or lower than base material [7]. It has been reported that, in 4 mm thick friction stir welded copper plates, nugget had lower hardness compared to base metal. Although grain size has been decreased, hardness reduction has been occurred slightly due to a reduction in dislocation density relative to the base metal [10]. On the other side, in FSW of 2 mm thick copper plates, nugget was harder than the base metal due to reduction in average grain size [11]. Microstructural evolutions during FSW process could certainly affect the mechanical properties. However, Shen et al. [13], reported that in pure copper, when welding speed increases, the size of nugget decreases and TMAZ become narrower, but the welding speed almost has no significant effect on the tensile properties of the joints when the welding speed varies in the range of 25–150 mm/min. Investigations on FSW of Cu–Zn brass alloys, particularly the influence of feed speed on microstructure and mechanical properties, are scarcely available [6,8–10,12]. It should be noticed that from economical point of view, using higher feed speeds is a favorable industrial demand [14].

The aim of this project is devoted to determine the effect of high feed speed on microstructure and mechanical properties of Cu–30Zn alloy. Macro- and micro-structures of weldment regions were characterized and compared by using optical microscopy (OM), scanning electron microscopy (SEM) and energy dispersive spectroscopy (EDS). In addition, hardness profile was measured through the weld zones. Elongation percentage (El%), yield

* Corresponding author. Tel./fax: +98 9151115085.
E-mail addresses: Sarvghad_madjid@hotmail.com, ma_sa89@um.ac.ir (M.S. Moghaddam).

0261-3069/$ - see front matter © 2011 Elsevier Ltd All rights reserved.
doi:10.1016/j.matdes.2011.01.015

strength (YS) and ultimate tensile strength (UTS) values were also obtained by performing tensile strength test on longitudinally specimens (with respect to weld center-line). Finally, the relationship between process variables, microstructure and mechanical properties will be discussed.

2. Experimental procedure

FSW process is carried out on Cu–30Zn brass plates of 300 mm (length) × 100 mm (width) and 5 mm of thickness. The chemical composition of the alloy is; 28.66% Zn, 1.54% Mn, 0.99% Al, 0.25% Ni, 0.19% Pb, 0.1% Fe, 0.034% Si and Cu as balance. Two work-pieces with square mating edges (butt joint) are clamped tightly on a 2 mm rigid carbon steel backing plate. This prevents the work-pieces from going apart or lifting up during the welding operation. The welding tool consists of a 15 mm diameter concave shoulder with coaxial circular treads and a conic pin of 4.9 mm length with parallel treads (Fig. 1a and b) and is made from H13 hot work steel. The probe is then rotated to a prescribed speed, 950 rpm, and tilted, approximately 2°, with respect to the work-piece normal axis. The tool is slowly plunged into the work-piece material at the butt line, until the shoulder forcibly contacts upper surface of the material and the pin is positioned in a short distance from the backing plate. A downward force is applied to maintain the contact and a short dwell time is observed to allow for the development of thermal fields for preheating and softening the material along the joint line. At this point, a lateral force is applied in the direction of welding (travel direction) and the tool is forcibly traversed along the butt, until it reaches the end of the weld (Fig. 1a and b). By using a manual milling machine including a gearbox system, four various feed speeds, 190, 235, 300 and 375 mm/min (namely: FS190, FS235, FS300, FS375), were chosen. In order to provide optical and SEM micrographs, cross-section of welded samples were wet polished up to 1200 grit SiC paper, degreased with acetone, washed with distilled water and finally dried with hot air. Etching was performed within $FeCl_3$ + HCl + H_2O solution. To visualize the macrostructure, macro-etching procedure was performed on both the cross-section and the sample extracted across the center-line of the weld zone. Tensile test was performed on longitudinal specimens using a ZWICK 250 kN instrument in accordance with ASTM E 8M-98 standard [15]. Hardness profile was measured along the top-line of the cross-section of the weldment using a Brinell hardness tester at a 10 kgf load and ball diameter of 1 mm. To assure the reproducibility, average value of five test results on samples was calculated and reported.

Macro- and micro-structural changes from the weld zone to the unaffected base metal are examined using a digital camera, OM and SEM (model: LEO 1450 VT) along the cross-section of all specimens.

3. Results and discussion

3.1. Macro- and micro-structural examinations

Fig. 2 shows the typical cross-sectional images of macro-etched FS300 and FS375 specimens. The joint exhibits three distinct microstructural regions, i.e. SZ at the weld center, TMAZ surrounding the SZ and base metal. A negligible HAZ also could be detected which has been reported previously by Meran [6]. Moreover, both retreating and advancing sides can be distinguished in the macrograph which is a characteristic of FSW process. Also, it can be seen that at 375 mm/min welding speed, a type of elongated defect, worm hole, is induced during the process due to the insufficient volume of material in the advancing side; see Fig. 2b.

Fig. 3 shows the sequence of grain size and microstructural variations from base metal to SZ of the welded material (specimen FS375) above the cross-section center-line. It can be seen that the grain size is gradually decreased by passing from base metal to SZ. In other words, in SZ, grain size is much smaller than in base metal. In comparison with base metal, well distributed, equiaxed and recrystallized grains are observed in SZ. While HAZ is negligible in all conditions, TMAZ, a mixture of small and larger size grains, is found in contact with base metal. Interestingly, a unique deformation pattern could be observed in SZ region (Fig. 3d). A similar pattern was also reported previously in friction stir welded copper alloy called "snake-like" pattern [13]. Apparently, this region is a spring-like band, mixed of ultra-fine grains and microporosities defined as "stir band". Particular influence of stir bands on the weld properties will be discussed in following sections.

A comparison between TMAZ and SZ microstructures for FS190, 235 and 300 specimens are illustrated in Fig. 4. Clearly, in TMAZ, due to several factors including thermal effects induced by the stirrer pin, nucleation of new grains (resulted from severe plastic deformation) and dynamic recrystallization phenomena, both fine and coarse grains are observed [1–2,12]; see Figs. 3 and 4.

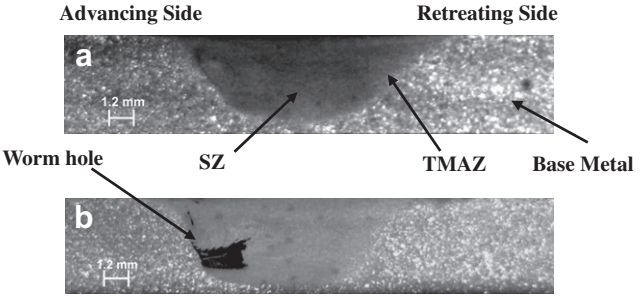

Fig. 2. Macrograph showing weld profile, (a) FS300 and (b) FS375.

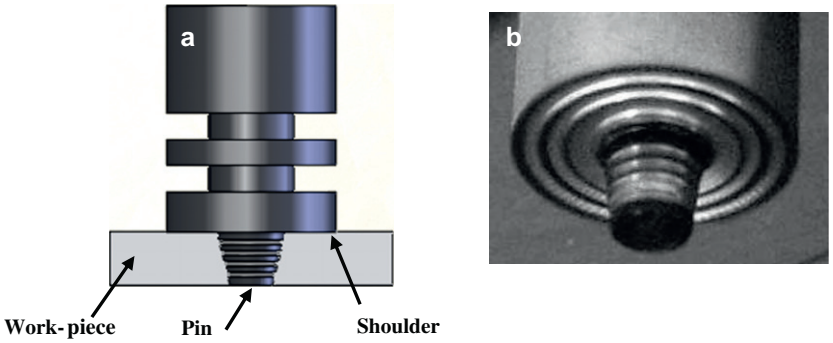

Fig. 1. (a) Schematic drawing of friction stir welding and (b) FSW tool used in this study.

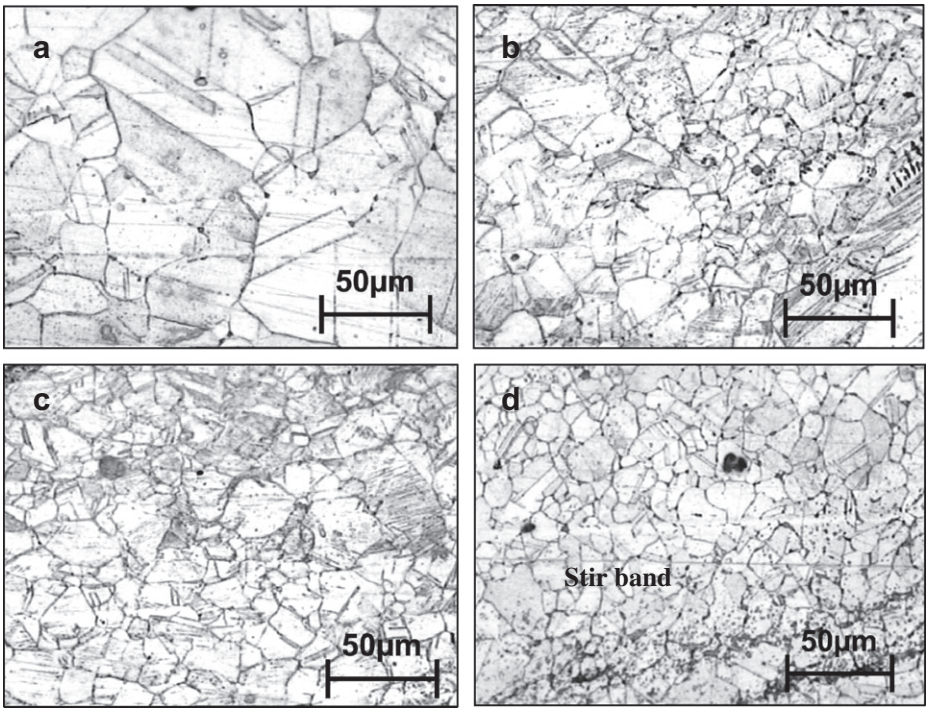

Fig. 3. OM images of the FS375 specimen cross-section showing microstructure spectrum from (a) base metal to (d) SZ including stir band. Transition region in (b) and (c) shows TMAZ.

In order to reveal the macrostructure in more details, the samples were immersed for 5 h in 2 M NaCl solution. Fig. 5a and b shows the cross-section (through the weld center-line) macrograph of FS235 and FS375 specimens. It can be observed that the stir bands extend and penetrate into more than two third of the plate thickness. The graphs also show the stir bands shape and density. It is evident that the density of stir bands increases by increasing in feed speed while their width decreases.

Fig. 6 shows grain size profile on the cross-section center-line of welds (typically measured from Figs. 3 and 4). Particular ultra-fine grain size, corresponding to stir bands, has not been taken into account. Generally, in all feed speeds, the grain size of about 40 μm in the base metal decreases to less than 7 μm in the SZ (a reduction of about 80%). Furthermore, as the welding speed increases from 190 to 375 mm/min, the average grains size in SZ does not change significantly. At first glance, this can be explained by the total heat input values. The total heat input, Q, generated by the FSW that affected the grain size can be simply expressed through the following equation [12,16]:

$$Q \propto \frac{R_s}{W_s} \tag{1}$$

where R_s is the tool rotation speed (rpm), W_s is travel or welding speed (mm/min) and Q refers to generated heat (J/mm). This implies that in this study the FSW heat input, Q, is inversely proportional to feed speed [12,16]. Since the grain size of single phase (α brass) in SZ does not show any distinct relationship with heat input, it seems that there must be another factor affecting grain size in SZ. As the heat input decreases (due to increase in welding speed), the amount of generated heat increases due to the rigorous plastic deformation. Therefore, these two concurrent opposing effects may balance each other as that the grain size in SZ does not change significantly by increasing in feed speed. As a conclusion, the grain size value in FSW depends both upon the heat input value and plastic deformation during the thermo-mechanical process.

Fig. 7 shows SEM/EDS analysis on an individual stir band for the FS375 specimen. Dark points represent micro-porosities formed in this zone. The SEM micrograph shows a mixture of fine round and elongated grains as a consequence of welding process, a characteristic of stir band region. Grain size measurement also revealed that the grain size in this region is approximately 1 μm which is considerably smaller than other regions even SZ with average grain size of 7 μm. EDS analysis performed at the vicinity of micro-porosities reveals the presence of mainly copper and zinc elements. A trace amount of iron and oxygen elements, as contaminations, could be also detected which can be attributed to the tool pin wear and oxides formation.

Fig. 8 shows the SEM microstructure of SZ (exactly beneath the shoulder) and TMAZ/base metal interface of FS375 specimen. Beneath the shoulder, Fig. 8a, severe plastic deformation pattern and some imperfections such as micro-porosities (maybe due to zinc evaporation and copper/zinc oxidation) could be observed. While the equiaxed grains are present in base metal, elongated and recrystallized grains are formed in TMAZ region, shown Fig. 8b.

3.2. Hardness

Plastic deformation in combination with the heat input also determines the mechanical properties (such as hardness) of friction stir welded specimens. Fig. 9 shows the hardness profile along the cross-section top-line of the welds performed at various feed speeds. Generally, the average hardness level decreases more than 30% by increase in feed speed. Although, the grain size does not vary significantly, decrease in hardness can be associated to the presence of induced imperfections such as worm hole and micro-porosities particularly generated in stir bands. This indicates that the hardness variations does not follow the grain size variation and deviates from the Hall–Petch mechanism which is different from the previous work on FSW of copper [13,17]. Increase in dislocation density, reduction in dynamic recrystallization (resulting an increase in residual stress), and induced imperfections caused

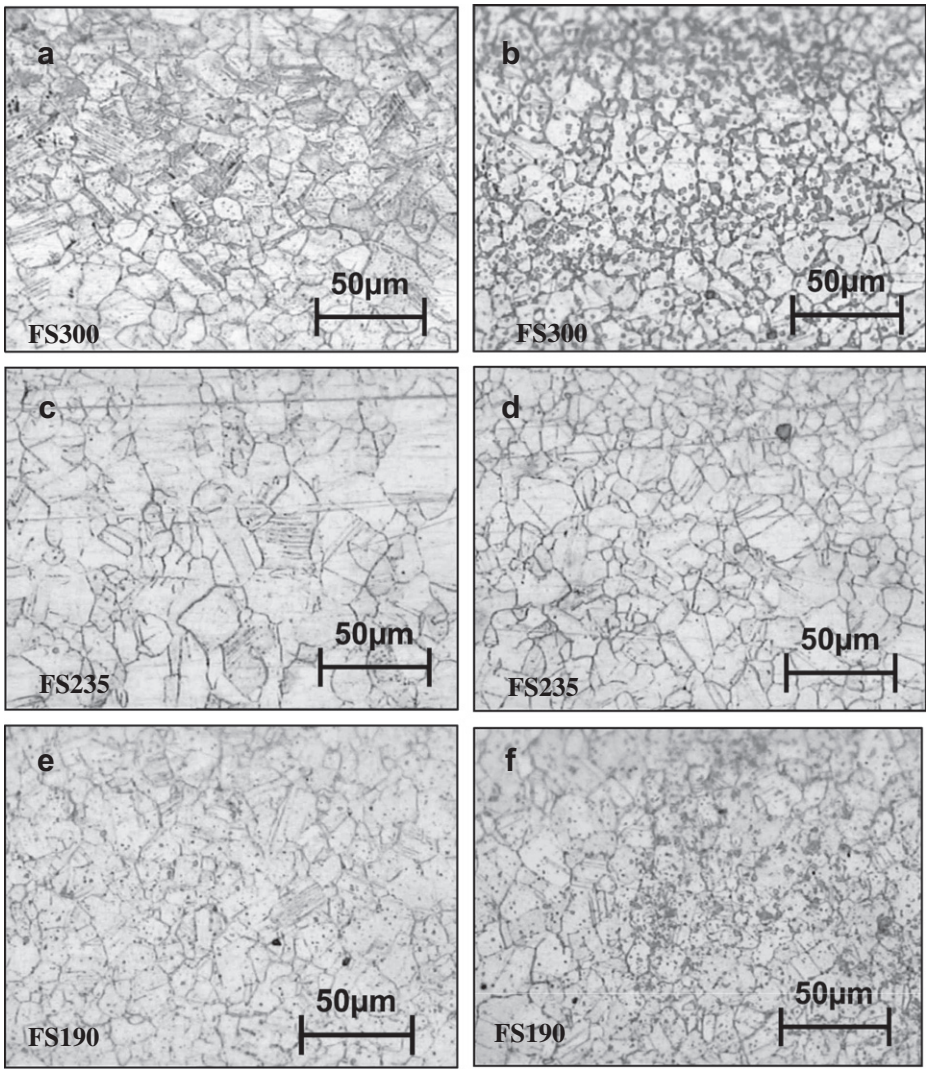

Fig. 4. Typical microstructures of the weld zone: TMAZ (left) and SZ (right).

by severe plastic deformation are all crucial mechanisms that affect the hardness values [10,16–20]. Where, friction and severe plastic deformation as two major sources for heat input, induce air entrapment beneath the shoulder as voids, zinc evaporation as micro-porosities and inclusions as copper/zinc oxides. Therefore, the hardness value is balanced by the Hall–Petch mechanism and plastic deformation influence.

Furthermore, hardness values within the weld zone in all welding conditions are slightly higher than that in the base metal, identical to the variations in trend of grain size, Fig. 6. Maximum hardness value can be attributed to the TMAZ, since it has a reasonable fine grain size and minimum imperfections in comparison with other regions. This can be seen as a slight increase in hardness value approximately at ±3 mm distance from the weld center-line in Fig. 9.

A trivial hardness difference could be observed between the retreating and advancing sides. The stress components in retreating and advancing sides have compressive and tensile characteristics, respectively. Consequently, advancing side has an inherent potential for creation of more imperfections such as worm hole [21–23]. Therefore, for a specific feed speed, retreating side shows higher values of hardness in comparison with the advancing side [1].

3.3. Tensile properties

Tensile properties of the welded specimens have been deduced from the stress–strain curves. The results were summarized in Fig. 10. For comparison, tensile properties of as received specimen are shown as zero feed speed. YS and UTS of all specimens increased slightly, in comparison with the as received specimen. Previous studies also showed that the decrease in heat input (i.e. increase in feed speed) improves the strength [16]. In the present study, despite decrease in hardness values, both YS and UTS values slightly increase by increasing in feed speed. It seems that a slight increase in tensile properties can be solely due to the stir band density and its width variations. As described before in Section 3.1, as feed speed increases, stir band density increases while its width decreases. Continues spring-like morphology of stir bands could act as a strengthening structure and increase in stir band density fairly improves the weld zone strength. An optimum feed speed, FS300, could be reported for the highest tensile strengths. However, YS and UTS values decrease at 375 mm/min feed speed most likely due to formation of defects.

It should be noticed that the variations in YS and UTS values are insignificant. On the contrary, by increasing in feed speed, elongation percentage diminishes remarkably from 57% in as received

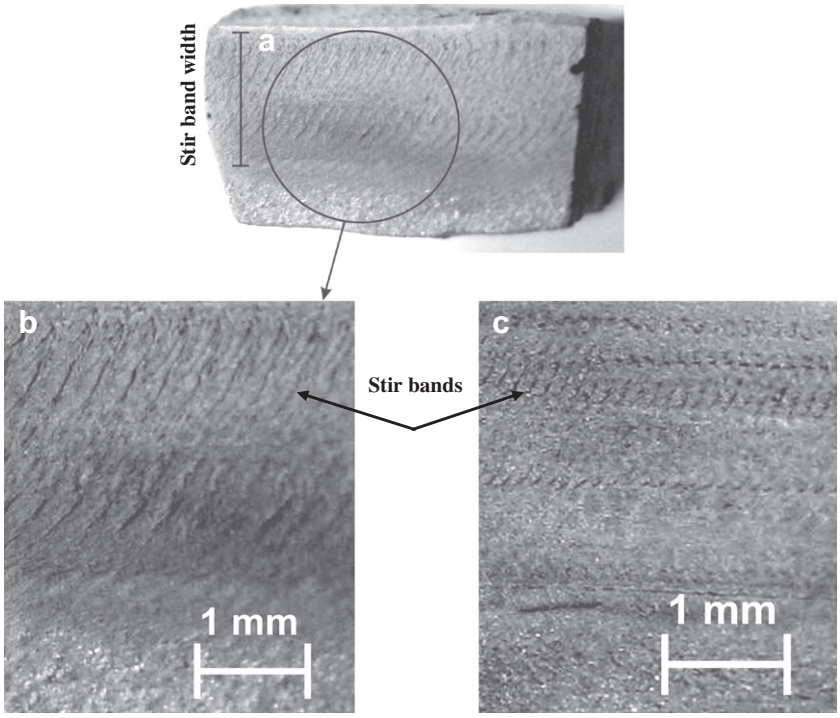

Fig. 5. Cross-section macrograph showing stir bands shape and density (normal to the direction of macrograph shown in Fig. 2), (a) and (b) FS235 and (c) FS375.

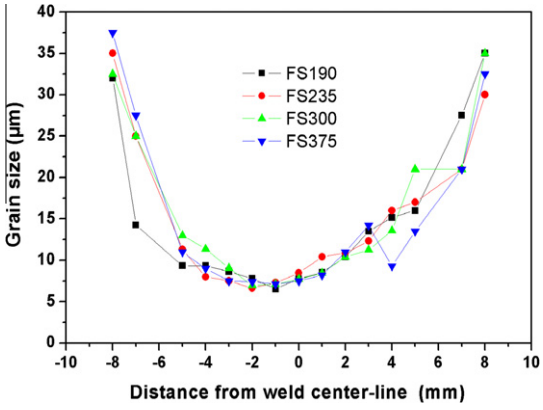

Fig. 6. Grain size variation from the base metal to the weld zone within the cross-section center-line of welds (rotation speed 950 rpm).

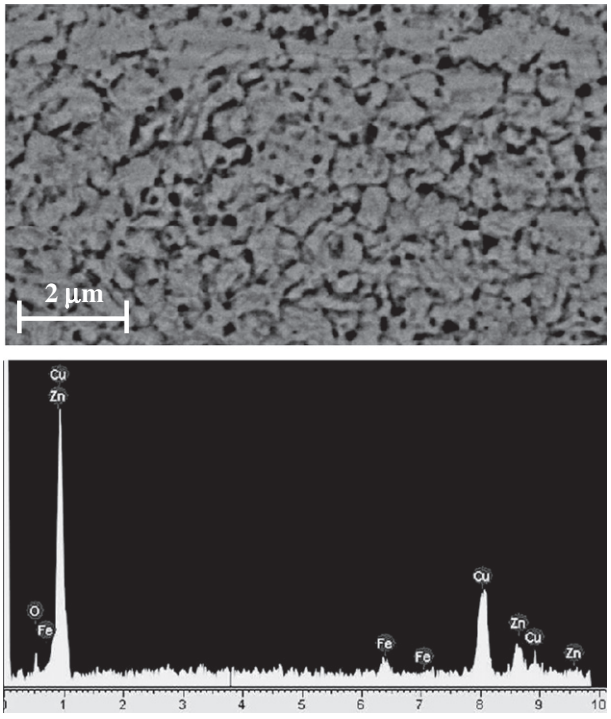

Fig. 7. SEM/EDS analysis of an individual stir band (FS375).

sample to a minimum of 27% in FS300 specimen, Fig. 10. Obviously, although existence of stir bands gives a minor improvement in strength but they reduce considerably the ductility due to their brittle structure in comparison with other microstructure constituents. The higher feed speed leads to the greater stir band density. Increase in stir band density leads to an increase in stress concentration (due to sever inhomogeneity between stir bands and the surrounding texture) and also causes deformation resistance. A slight increase in ductility in FS375 specimen may be attributed to the higher amount of compressive residual stress in comparison with FS300 specimen. Indeed, as feed speed increases, strain rate and consequently the compressive residual stresses and defect formation tendency increase.

Fig. 11 represents the specimens' macrograph after longitudinal tensile test. Interestingly, fracture occurs along stir bands normal to welding direction. This can be evidence for the important role of stir bands on mechanical behaviour of friction stir welded brass. The snake-like crack pattern can be associated to the stir band morphology. By increase in feed speed, the crack density also increases, similar to the trend of stir band density. To precisely identify the origin of crack initiation, a SEM image at SZ/stir band interface was obtained, shown in Fig. 12. Surprisingly, the crack originates exactly adjacent to a stir band, confirming the proposed mechanism based on stir band influence. A recent study conducted on corrosion behaviour of friction stir welded copper plates revealed that stir band also has a crucial effect on corrosion

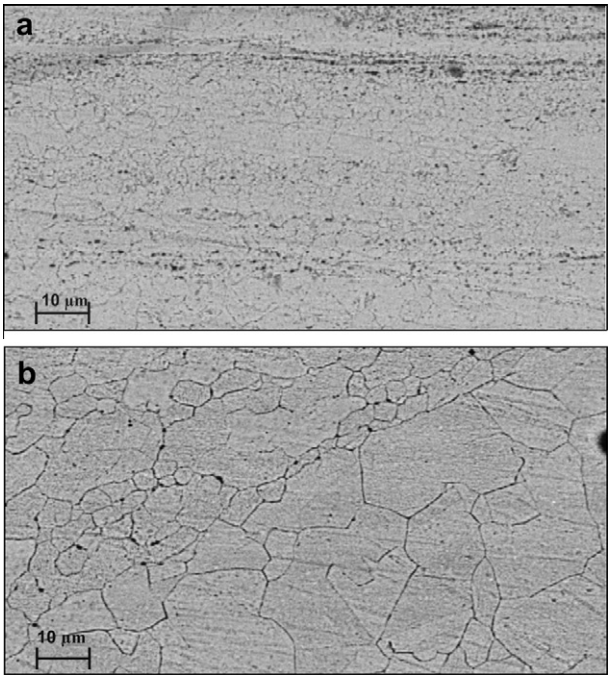

Fig. 8. SEM microstructure of (a) SZ and (b) boundary region between TMAZ and base metal.

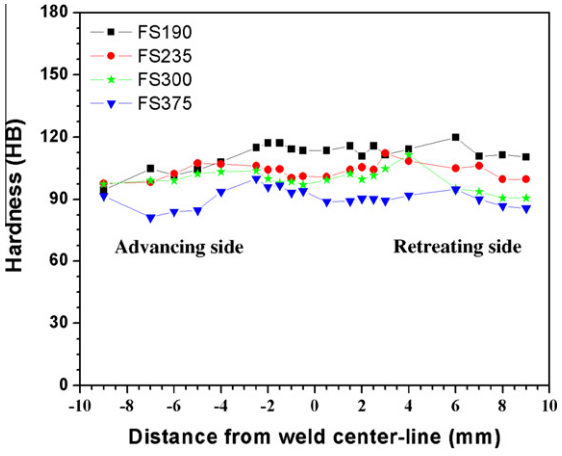

Fig. 9. Hardness distributions along the top-line on the cross-section of welds.

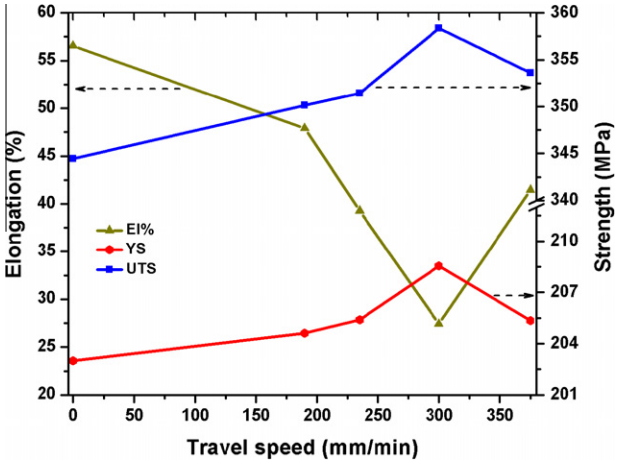

Fig. 10. YS, UTS and elongation percentage of longitudinal tensile weld and as received specimens.

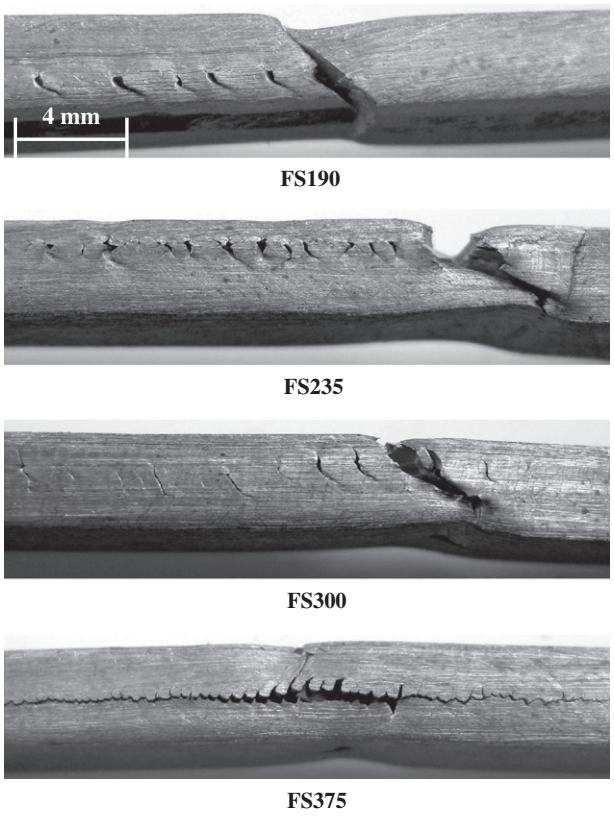

Fig. 11. Macrographs of longitudinal tensile test specimens showing stir bands after fracture.

initiation. It was observed that local corrosion attacks were preferably taken place at stir bands [24].

In summary, at a constant grain size, strength and ductility have reverse correlation. Up to the 300 mm/min feed speed, the strengthening mechanism of stir bands overcomes its weakening characteristic by crack initiation at stress concentration sites. At higher speeds, the weakening characteristic mechanism overcomes the strengthening mechanism as a result of significant increase in crack initiation sites. Therefore, it can also be concluded that the mechanical properties are definitely affected by formation and morphology of the stir bands.

4. Conclusions

In this study, the effect of 190–375 mm/min feed speeds on the microstructure and mechanical properties of friction stir welded Cu–30Zn alloy was investigated. The main conclusions summarized as below:

(1) FSW causes formation of equiaxed, well distributed and recrystallized grains in SZ and some coarser grains in the TMAZ.
(2) A unique deformation pattern could be observed in SZ region. This region is a spring-like band, mixed of ultra-fine grains and micro-porosities defined as "stir band" which has a significant influence on weld properties. Stir band density increases by increase in feed speed.
(3) The grain size value in FSW depends upon the concurrent effect of heat input and plastic deformation during the thermo-mechanical process. The grain size profile was independent of feed speed.

Fig. 12. SEM image at stir band/SZ interface.

(4) The hardness value decreases by increase in feed speed and balanced by the simultaneous Hall–Petch mechanism and plastic deformation.
(5) Increase in feed speed leads to a slight improvement of YS and UTS, associated to continuous spring-like morphology of stir bands acting as a strengthening structure. However, ductility reduces considerably from 57 to 27% due to stir band brittle structure. The higher the feed speed, the greater the stir band density. Therefore an increase in stress concentration and consequently deformation resistance, occurs
(6) It is observed that during tensile test, fracture cracks originate exactly adjacent to the stir band.

Acknowledgements

Ferdowsi University of Mashhad and Khorasan Science and Technology Park (KSTP) are acknowledged for financial support and providing experimental facilities.

References

[1] Mishra RS, Ma ZY. Friction stir welding and processing. Mater Sci Eng R 2005;50:1–78.
[2] Khaled T. An outsider looks at friction stir welding. Federal aviation administration; 2005. [R No ANM-112N-05-06 (<www.faa.gov>)].
[3] ASM Handbook. Powder metal technologies and applications. 2nd ed. vol. 7. New York: ASM international; 1998. [p.752–63].
[4] Biro E, Weckman DC, Zhou Y. Pulsed Nd: YAG laser welding of copper using oxygenated assist gases. Metall Mater Trans A 2002;33:2019–30.
[5] Oates WR. Welding handbook: Materials and applications. 8th ed. vol 3. Miami: AWS; 1972. [p. 181].
[6] Meran C. The joint properties of brass plates by friction stir welding. Mater Des 2006;27:719–26.
[7] Nandan R, DebRoy T, Bhadeshia HKDH. Recent advances in friction stir welding–process, weldment structure and properties. Progress in Materials Science 2008;53:980–1023.
[8] Liu HJ, Shen JJ, Huang YX, Kuang LY, Liu C, Li C. Effect of tool rotation rate on microstructure and mechanical properties of friction stir welded copper. Sci Technol Weld Join 2009;14:577–83.
[9] Xie GM, Ma ZY, Geng L. Development of a fine-grained microstructure and the properties of a nugget zone in friction stir welded pure copper. Scripta Mater 2007;57:73–6.
[10] Lee WB, Jung SB. The joint properties of copper by friction stir welding. Mater Lett 2004;58:1041–6.
[11] Sakthivel T, Mukhopadhyay J. Microstructure and mechanical properties of friction stir welded copper. J Mater Sci 2007;42:8126–9.
[12] Park HS, Kimura T, Murakamic T, Nagano Y, Nakata K, Ushio M. Microstructures and mechanical properties of friction stir welds of 60% Cu–40% Zn copper alloy. Mater Sci Eng A 2004;371:160–9.
[13] Shen JJ, Liu HJ, Cui F. Effect of welding speed on microstructure and mechanical properties of friction stir welded copper. Mater Des 2010;3:3937–42.
[14] Hautala T, Tianien T. In: Proceedings of the sixth international conference on trends in welding research, pine mountain, GA, ASM International; 2003. p. 324.
[15] ASTM E 8M: Standard Test Method for Tension Testing of Metallic Materials. ASTM International; 1998. p. 8.
[16] Frigaard O, Grong O, Bjorneklett B, Midling OT. In: Proceedings of the 1st international symposium on friction stir welding, Thousand Oaks, CA, USA; 14–16 June, 1999.
[17] Brooks CR. Heat treatment, structure and properties of nonferrous alloys. 2nd ed. vol. 275–327. American Society For Metals; 1984. [p. 21–49].
[18] Dieter GE. Mechanical Metallurgy. 3rd ed. McGraw-Hill; 1976.
[19] Kelly A, Groves GW, Kidd P. Crystallography and crystal defects. 2nd ed. John Wiley and Sons; 2000. p. 257–265.
[20] Hull D, Bacon DJ. Introduction to dislocations. 4th ed. Oxford OX28DP: Linacre house, Jordan Hill; 2001. [p. 82–101].
[21] Leal R, Loureiro A. Defect formation in friction stir welding of aluminum alloys. Adv Mater Forum II 2004;299–302:455–6.
[22] Guerra M, Schmidt C, McClure JC, Murr LE, Nunes AC. Flow patterns during friction stir welding. Mater Charact 2002;49:95–101.
[23] Schmidt H, Hattel J. A local model for the thermomechanical conditions in friction stir welding. Model Simul Mater Sci Eng 2005;13:77–93.
[24] Parvizi R, Moayed MH, Davoodi A, Haddad sabzevar M. Galvanic corrosion behavior of friction stir welded copper alloy in 3.5% NaCl. 216th ECS Meeting, abstract no. 1680, Vienna, Austria; 4–9 October, 2009.